Received: 5 March 2023 | Revised: 22 April 2023 | Accepted: 25 May 2023

DOI: 10.1002/ecs2.4604

ARTICLE

ECOSPHERE
AN ESA OPEN ACCESS JOURNAL

# Estimating wolf (*Canis lupus*) densities using video camera traps and spatial capture–recapture analysis

**José Jiménez**[1] | **Daniel Cara**[2] | **Francisco García-Dominguez**[3] | **Jose Angel Barasona**[4]

[1]Instituto de Investigación en Recursos Cinegéticos (IREC, CSIC-UCLM-JCCM), Ciudad Real, Spain

[2]TRAGSATEC, Madrid, Spain

[3]Ministerio para la Transición Ecológica y el Reto Demográfico, Madrid, Spain

[4]VISAVET Health Surveillance Centre & Animal Health Department, Faculty of Veterinary, Universidad Complutense Madrid, Madrid, Spain

**Correspondence**
José Jiménez
Email: jose.jimenez@uclm.es

**Funding information**
Ministerio para la Transición Ecológica y el Reto Demográfico (MITECO)

**Handling Editor:** Jesse Lewis

## Abstract

Estimating population density is critical for effective species conservation, wildlife management planning, and long-term monitoring. Obtaining accurate estimates is especially important for the wolf (*Canis lupus*), a widely distributed northern hemisphere apex predator whose management and conservation are highly controversial in most of its range, and whose presence usually generates high-profile media coverage. The peculiarities of wolf social spatial organization and behavior can violate the assumptions of capture–recapture models (uniformity and independence, respectively) to a greater or lesser extent and make it difficult to obtain precise and reliable density estimates. This paper presents a case study, which estimated the population density of the Iberian wolf in the Dorsal Gallega mountain ridge (Galicia, NW Spain) based on the identification of individual wolves from their traits and behavior using video camera traps and spatially explicit capture–recapture (SCR) analyses. The study followed three phases. Firstly, field data were collected by installing camera traps and changing their location until the entire area was sampled. Second, a complete morphological and behavioral study of the wolves recorded was performed to facilitate individual recognition. Third, overdispersion due to gregariousness and other sources of heterogeneity was modeled in the SCR analyses comparing Poisson and negative binomial observation models with different random effects on the baseline detection probability. We estimated a density of 2.88 (SD: 0.37) wolves/100 km$^2$ in the study area. We concluded that estimating wolf population size using camera trap videos, individual identification, and SCR provides a feasible method and can be used for estimating the density in similar species.

**KEYWORDS**
camera trap, *Canis lupus*, gregariousness, heterogeneity, identification, population density, spatial capture–recapture, video, wolf

## INTRODUCTION

Estimating the abundance of wildlife populations is an essential part of ecological research, monitoring, and management (Williams et al., 2002). Density is one of the most useful parameters, since it establishes a connection between the number of individuals in a population and the space they occupy, allowing the spatial design and implementation of management activities and monitoring in an area. Spatially explicit capture–recapture (SCR) models allow estimates of population density by modeling capture probability as a function of the distance between activity centers and detectors (Efford et al., 2004; Royle & Young, 2008) using spatial information derived from the detector coordinates. SCR methods overcome some of the limitations of nonspatial capture–recapture models and allow inferences regarding the location of animal activity centers, enabling better spatial design of management activities (Havmøller et al., 2019; Jiménez et al., 2017).

However, SCR methods based on noninvasive and relatively inexpensive sampling techniques, such as camera-trapping, are more difficult to apply to species with cryptic morphologies. If the target species is also gregarious (species that live in groups), the application of the SCR model may become even more methodologically challenging, as the model's assumptions that individuals are (1) uniformly distributed in space and (2) independently detected when using detection devices (e.g., camera traps) are likely to be violated (Royle et al., 2014, p. 150). Using simulations of wolf (*Canis lupus*) populations based only on the grouping of their activity centers, López-Bao et al. (2018) suggested that their spatial aggregation resulted in only a slight underestimate of density. However, Bischof, Dupont, et al. (2020) showed that both the aggregation of activity centers (lack of spatial uniformity) and the cohesion or synchrony of detection patterns of members of a group (lack of detection independence) affected the accuracy of SCR model results. They concluded that SCR models are only robust at moderate levels of individual aggregation and cohesion. Their simulations over the entire habitat sampled were characterized by a similar absence of bias and changes in precision at low and moderate levels of aggregation, regardless of the level of cohesion. They used a maximum likelihood estimation approach to develop an overdispersion factor ($\hat{c}$) to correct the estimated parameter variance. Emmet et al. (2022) developed a cluster SCR model to estimate group density, individual density, and group size, using a case study on African wild dogs (*Lycaon pictus*). Lastly, Dey et al. (2023) described and simulation-tested three Bayesian SCR models that used generalized linear mixed models to account for latent heterogeneity in the baseline detection rate across detectors, using independent and spatially autocorrelated random effects and a two-group finite mixture model.

Despite these methodological developments, the application of SCR to the wolf, a gregarious species with a key role as a top predator in trophic cascades (Newsome & Ripple, 2015; Ripple & Beschta, 2012; Ripple et al., 2001), remains a challenge, and studies using empirical data are very scarce. Wolf population size estimates have usually relied on expensive noninvasive genetic techniques (Bischof, Milleret, et al., 2020; López-Bao et al., 2018; Mattioli et al., 2018; Roffler et al., 2019). To our knowledge, no SCR methodological developments have been applied to this gregarious species to improve the results obtained from inexpensive and relatively easily gathered camera trap data.

In this study, we used video recordings of wolves obtained from camera traps in Galicia (NW Spain). The recordings allowed identification of individual wolves based on their morphological characteristics, mange lesions, and behavior. To account for the effect of gregariousness on observations and other sources of heterogeneity, we used an SCR model to analyze the data with Poisson and negative binomial observation models with different random effects on the baseline detection rate and tested its goodness of fit (GoF). We show that this approach can provide a reliable means for estimating the population size of this species, which could also be applied to other species with similar characteristics.

## METHODS

### Study area

The study area (Figure 1) is located in the Dorsal Gallega mountain ridge (Pontevedra province), a group of mountain ranges running from north to south through central Galicia (NW Spain). The altitude varies around 500 m, with nearby peaks of 1100 m. The annual average rainfall is 2459 mm. Moorland, with *Erica* spp. and gorse (*Ulex* spp.), predominates on the high plateaus as a result of human activity, although there are some patches of native forest (*Quercus robur*) and coppices on the slopes. Roe deer (*Capreolus capreolus*) and wild boar (*Sus scrofa*) are abundant in the region. The human population density is moderate, 25.4 inhabitants/km$^2$, and declining (INE, 2018). The main land use is extensive livestock (cattle, sheep, and horses) farming. Previous information on wolves in the area was given in the 2013–2014 National Wolf Survey (MITECO, 2015), and four packs or territorial social groups (Mech & Boitani, 2006) were detected, based on surveys of signs, howling sessions, and other information (Jiménez et al., 2016).

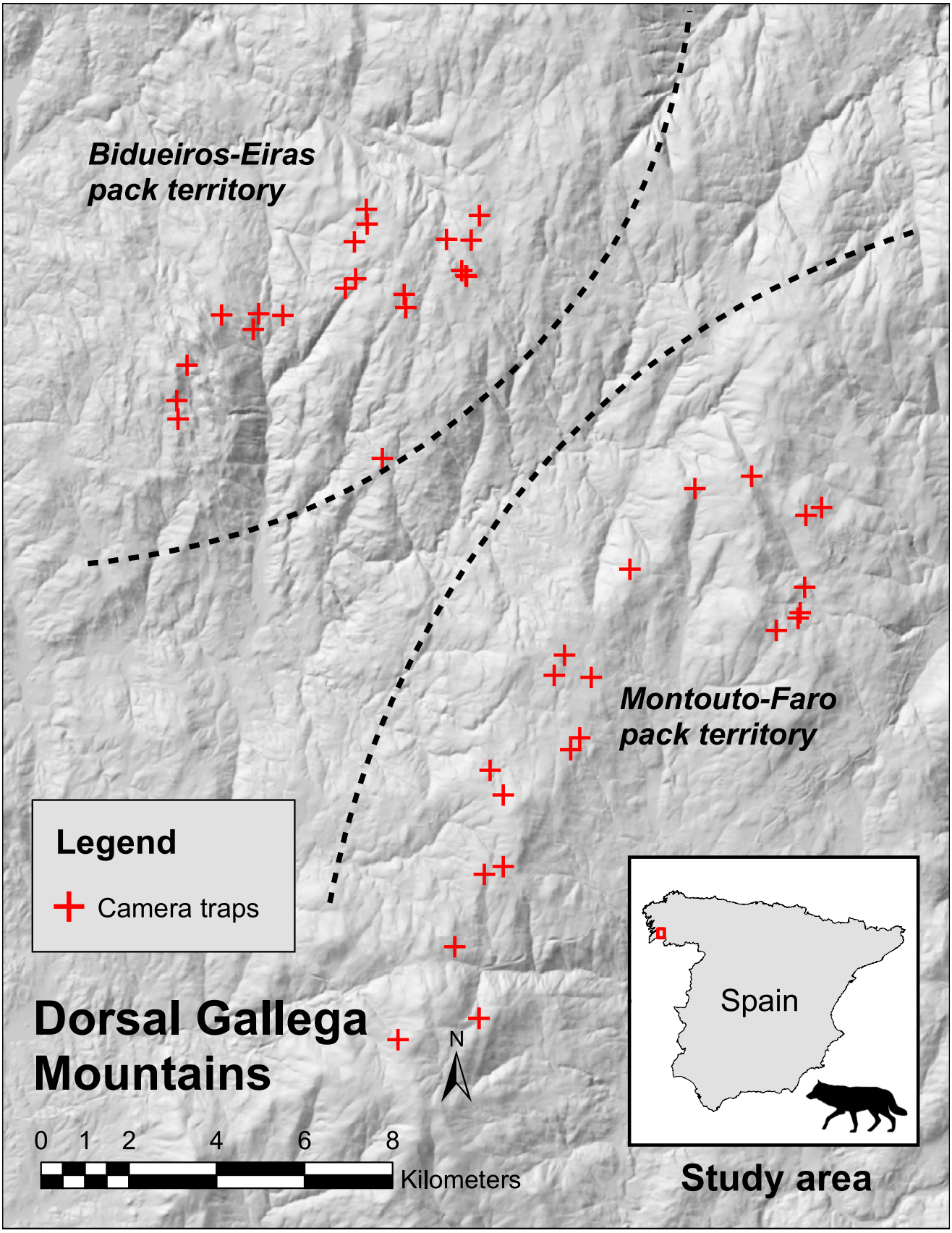


**FIGURE 1** Map of the study area in the Dorsal Gallega mountain ridge. The study area was located in Pontevedra (Galicia, NW Spain) and was monitored using 43 camera-trapping sites. The inset map shows the location of the study area in Spain (red rectangle).

The closest packs identified were located approximately 10 km from our study area.

## Sample collection

The wolf population in the area was monitored using camera traps (Moultrie M-990i; Birmingham, AL, USA). The study covered 119 days during summer and autumn (June 4, 2015–September 30, 2015). Twenty camera traps were used, installed at a height of 70 cm on fences, stonewalls, and trees along trails and at road junctions. Trap locations were changed during the study to sample the whole area. Forty-three different trap locations were used (Figure 1). The resulting polygonal envelope covering all of the camera trap locations was 28,022.7 ha in size. Wolves were attracted to the cameras using rotten fish extract scent lures (Bullard, 1982). The attractant was sprayed once only per camera trap, on stones and soil 3–4 m away from the trap or allowed to soak into porous materials such as logs. The traps were set to trigger a photograph and a 20-s video. An "event" was defined as the presence or detection of an animal within a camera trap field of view (Jumeau et al., 2017). The minimum interval between events to be considered independent was 30 min. Where several animals were "captured" in a single picture, each individual wolf constituted a separate event.

## Individual identification

We used observable anatomical or pathological features to identify individual wolves captured in the video events. From these, we compiled a catalog of the identifiable individuals and gave each a descriptive name (in Galician) for reference in this study. The main recognition characters used were gender, age class (adults/subadults and pups), behavior, morphological features (body, tail, and head sizes; length-to-height ratio; development of mammary glands), phenotypic characters (color; size; density of hair in different part of the body), anatomical peculiarities (congenital; acquired deformities), and pathological peculiarities (alopecia; lameness; inflammation; wounds) (Figure 2; Appendix S1). Lesions compatible with sarcoptic mange—a parasitic skin infection caused by *Sarcoptes scabiei*—were also important distinctive features owing to the wide variety of long-term marks observed on the skin and hair. Sarcoptic mange has been reported in Iberian wolves in northern Spain (Domínguez et al., 2008), and camera trap data have previously described it as a useful means of monitoring its occurrence and temporal trends in wolf populations (Oleaga et al., 2011). The videos allowed the identification of mange-compatible lesions: alopecic zones and erythema with active inflammatory borders can be clearly seen. Because such lesions are temporary, they cannot be used over an extended period but are perfectly suited for identifying individuals over a short period, such as that in this study. We compiled catalogs of photographs extracted from the videos and made visual comparisons among all of the photographs obtained to identify individual wolves where possible. Although individuals could be identified from both day and night photographs, photographs from daytime videos facilitated morphological study of individuals for catalog and comparisons with other videos due to their better quality and sharpness. To highlight the importance of daytime video in the identification process and as a reference for future work, we showed wolf activity pattern from all capture events using the overlap package (Ridout & Linkie, 2009) in R (R Core Team, 2022).

Although individuals could be recognized in most of the videos, there were those in which individual identification was not possible (e.g., blurred images or individuals behind others). Such cases were termed "data reduction," "dilution," or "subsampling." This situation is common in other scientific studies, such as in genotyping (where a sample contains insufficient markers). We assumed that, if the number of recaptures was sufficient (Efford et al., 2004), and data reduction was random, this data reduction would only affect the basal detection rate ($\lambda_0$, the expected detection rate when the center of activity coincides with the detector) and not the population size estimate (Murphy et al., 2018). As our dataset had a high cumulative probability of capture for each individual, which is uncommon in SCR studies, we tested how the precision and bias of the model estimates changed progressively as more samples were lost to misidentification. We "diluted" our SCR data in three trials in which 60%, 40%, and 20% of the total detections were used from the model at random, to evaluate the relationships between sample size and root-mean-square error (RMSE) and relative bias (RB) for the estimates of $D$ and $\sigma$. The posterior point estimates of the selected model using all of the SCR data were used as a comparative reference. For each trial, we simulated 100 different datasets, using a binomial distribution for random data dilution.

The total number of wolves (with and without identification) appearing in all camera trap video captures per day was used as a proxy for pack cohesion, assuming that the number of individuals appearing in any one video capture is an underestimate of the actual number present in the vicinity of the camera. The aggregation of all events observed in the videos per camera trap and day should report behavior that, although temporally separated, could indicate pack cohesion.

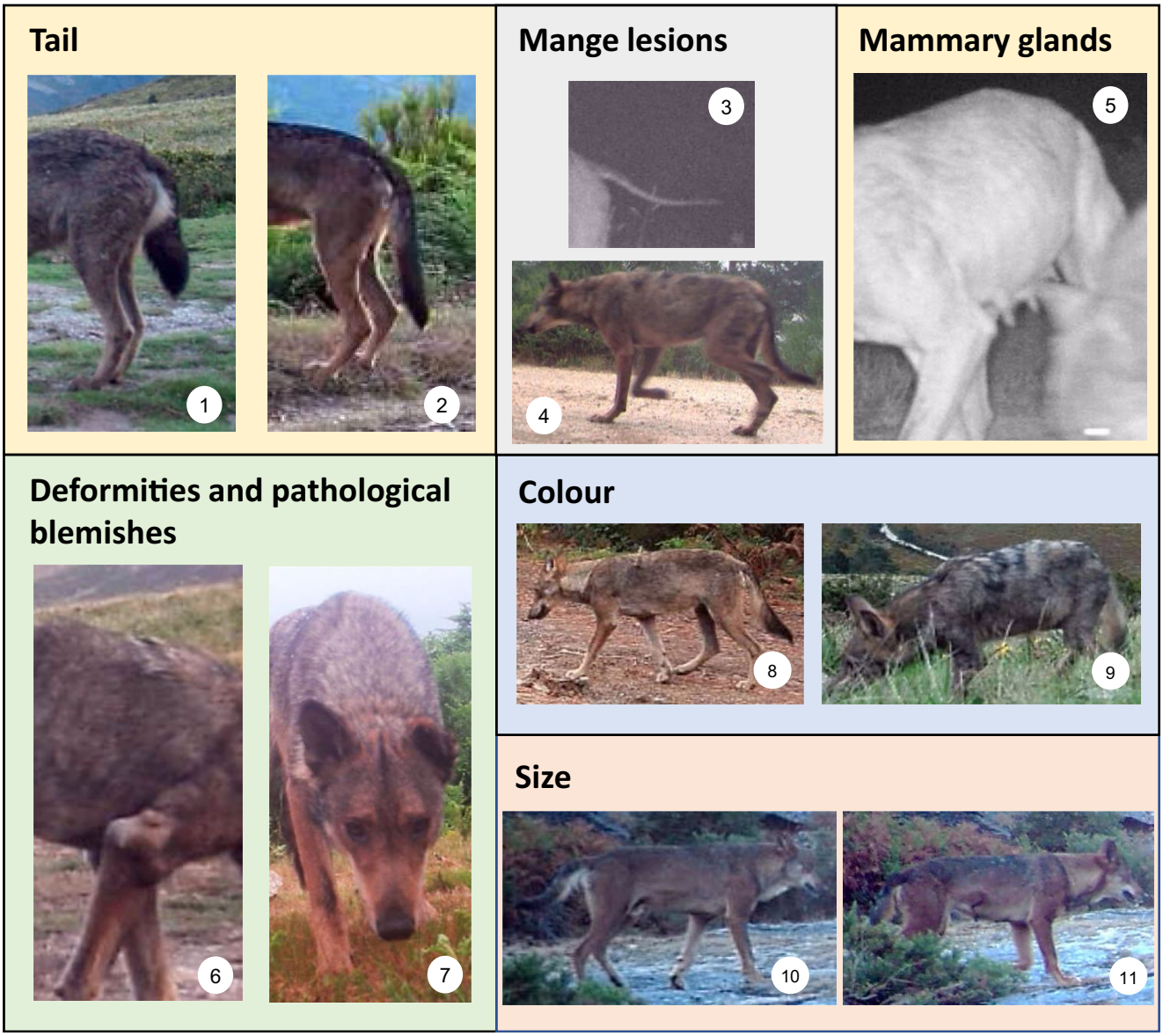


**FIGURE 2** Individual identification of wolves using video camera traps. The traits used include tail sizes, body shape, and hair density (1: *Pequeno* and 2: *Pardellas*); pathological blemishes, for example, alopecia due to mange lesions (3: *Eira* and 4: *Pinta*); development of mammary glands (5: *Deva*); anatomical deformities (6: *Telleira* and 7: *Jicho*); and phenotypic characteristics, for example, color (8: *Clara* and 9: Montouto-Faro pup number 1) and size (10: *Foxo* and 11: *Laxe*) (the photograph shows the greater height of the male compared with the ground surface and the height of the vegetation in the background). For complete information, see Appendix S1 (all images are taken from video camera traps set by the authors).

## Population density estimates

To address the lack of independence in individual detections, our working hypothesis was that aggregation and pack cohesion would lead to heterogeneity. Due to aggregation and cohesion, many detectors would register no detections, and those that did would detect more than the model prediction. A priori, one would expect that heterogeneity by individual-by-trap-by-occasion would be the most relevant for this group-living species. However, we may also find other sources of heterogeneity, e.g., individual heterogeneity in detection due to different behavior. We considered models with Poisson (P) and negative binomial (NB) observation models and different random effects on the baseline detection rate to explore relevant sources of heterogeneity. Assuming that cohesiveness in wolf packs is related to their ability to kill larger prey and improve their competitive ability against scavenging animals (Schmidt & Mech, 1997; Vucetich et al., 2004), we would predict that pack cohesion in our study area would be medium/low, given that the main food source in the area consists of small prey and

medium-sized domestic livestock. The effects of overdispersion should therefore be minimal according to Bischof, Dupont, et al. (2020) and could be addressed using random effects (Harrison, 2014; Kéry & Schaub, 2012, p. 82) or NB observation models (Cove et al., 2023).

We used a Bayesian SCR (Royle et al., 2014) approach in Nimble (de Valpine et al., 2017, 2022) and R (R Core Team, 2022). The standard SCR model assumes that individual activity centers $i = 1,2,...,N$ are distributed over a region or state space $(S)$ and that individuals are sampled by our camera trap array within $S$. The distribution of individual activity centers, $s_i = (s_{i_1}, s_{i_2})$, is described here by a homogeneous point process, such that $s_i \sim \text{Uniform}(S)$. The activity centers are latent variables to be estimated by the model given the trap-specific events for the $n$ detected individuals at traps $j = 1,2,...J$ with locations $x_j = (x_{j_1}, x_{j_2})$. Assuming that detection frequencies are a decreasing function of the distance $d_{ij}$ between an individual activity center $s_i$ and a camera trap location $x_j$, the expected detection rate (1) can be defined as:

$$\lambda_{ij} = \lambda(s_i, x_j) = \lambda_0 \times \exp\left(\frac{-{d_{ij}}^2}{2\sigma^2}\right), \quad (1)$$

where $\lambda_0$, the basal detection rate, is the expected detection rate when $d_{ij} = 0$, indicating direct overlap of an activity center with a trap; and $\sigma$ is the scale parameter of the half-normal detection function.

The detection rate can covary, for example, with the trapping occasion for sampling efforts with multiple occasions (e.g., $\lambda_{ijk}$ for $K > 1$). We assumed that the event histories of the $N$ observed individuals followed a Poisson (P) (2) or negative binomial (NB) (3) probability distribution of counts. The latter is considered adequate to describe aggregate event patterns (Anscombe, 1950) and has been previously used by Cove et al. (2023) in SCR observation models to deal with overdispersion in detection.

We used data augmentation to estimate the number of unobserved individuals (Royle et al., 2007). We augmented the $n$ observed detection histories with $M - n$ "all-zero" histories, choosing a value such that $M \gg N$, and the likelihood for the zero-inflated true detection frequencies $y_{ijk}$ was then conditioned on a partially latent binary indicator variable $z_i$ that describes the membership of individual $i$ in the population (2 and 3):

$$y_{ij} | z_i \sim \text{Poisson}(\lambda_{ij} \times K \times z_i), \quad (2)$$

$$y_{ij} | z_i \sim \text{Negative Binomial}(\lambda_{ij} \times z_i, r \times K), \quad (3)$$

where $r$ is the size parameter from the NB distribution. Where there is no variation in $K$, we aggregate the observed number of encounters in each trap over the $K$ sample occasions for more efficient computation (the sum of NB random variables is NB with $\text{size} = \text{size}_1 + \text{size}_2 + \cdots + \text{size}_n$) simplifying the detection model (2 and 3) as in Cove et al. (2023).

$\Pr(z_i = 1) = 1$ for the $n$ observed individuals, and $z_i \sim \text{Bernoulli}(\psi)$ for the entire collection of $M$ individuals. The population size can then be derived from the sum of indicators, $N = \sum z_i$ (realized $N$) or from the product $M \times \psi$ (expected $N$), and the density, $D$, can be derived by dividing the population size by the area of the state space, such that $D = N/\|S\|$.

To deal with the overdispersion, we used different random effects on the basal detection rate, following a common normal distribution (4):

$$\text{Normal}\left(\mu_0, \sigma_p^2\right), \quad (4)$$

where $\mu_0$ is the log-scale mean with a variance $\sigma_p^2$.

We compared (1) Poisson observation (P) model with a constant baseline detection rate as a null model; (2) P-$\varepsilon_i$: random effect on detection rate by individual; (3) P-$\varepsilon_j$: random effect by trap; (4) P-$\varepsilon_{ij}$: random contribution from each individual-by-trap combination; and (5) P-$\varepsilon_{ijk}$: random contribution from each individual-by-trap-by-occasion combination. We also compared (6) negative binomial observation (NB) model, which is actually a Poisson model where the random effects have a Gamma distribution, with a constant baseline detection rate; and (7) NB-$\varepsilon_j$: trap-level random effect on baseline detection rate. We thus compared different observation models and random effects. To save computation time, we used a "zero's trick" to buffer an irregular trap array without discretizing the state space (R. Chandler, public communication, see R+Nimble code). Posterior probabilities were calculated using three independent Markov chain Monte Carlo (MCMC), with 125,000 iterations each, and a burn-in of 25,000 iterations, thinning by five. We assessed the MCMC convergence and mixing by visually inspecting trace plots and then calculated the Gelman–Rubin statistic (R-hat <1.1) (Gelman et al., 2013) using the R package coda (Plummer et al., 2006). We used model selection by widely applicable information criterion (WAIC; Watanabe, 2013) to rank the fit of the candidate models using MCMC and then used the GoF of the models to diagnose severe violations of the model assumptions, and hence reduce the risk of drawing erroneous inferences (Pradel et al., 2005), by computing the Bayesian $p$ value (BPV) based on measures of the systematic dissimilarity between the observed data and posterior predictive distribution of the data (Gelman et al., 1996). Thus, the computation of BPVs requires the specification of a discrepancy measure by

choosing the aspects of the model to be checked. Following Royle et al. (2014, p. 232), we selected three statistics to evaluate the observation model: (1) individual per detector frequencies; (2) individual detection frequencies; and (3) trap detection frequencies. GoF was calculated using three independent MCMC simulations, with at least 50,000 iterations each, and a burn-in of 10,000 iterations, but in P-$\varepsilon_{ijk}$, due to the computational intensity we expected in generating BPV distributions, we limited to 10,000 iterations and a burn-in of 5000 iterations. To estimate and compare the population sizes ($N$) estimated by each model, a buffer of exactly $3\times\hat{\sigma}$ was set around the camera trap grid area, using the $\hat{\sigma}$ value obtained from a previous MCMC run. In the data dilution simulations, we used three chains, with 5000 iterations each, and a burn-in of 1000 iterations, thinning by five. We reported the posterior mode for point estimates (SD), unless clearly stated otherwise.

## RESULTS

Camera traps were active for 1889 day-traps (Appendix S2: Figure S1) in 43 locations (Figure 1). The wolves were very attracted to the rotten fish extract bait provided and often rubbed themselves against the bait or rolled on it, which allowed direct observation of their sexual organs helping with individual identification. We obtained 802 wolf events, 562 with identification (an average of 22.5 events/individual) and discarded 240 events where an identification could not be made. We recorded 527 recaptures. Of the spatial recaptures (the same wolf detected at different traps), two wolves were detected in 11 cameras; two in 10; two in 9; two in 8, two in 7; one in 6; one in 5; two in 4; one in 3; nine in 2; and one in 1 camera. We identified 25 individuals in the photo and video captures (Appendix S1) in two packs whose aggregate activity centers of pack members were 11.4 km apart, as depicted using the spiderplot function of the scrbook package (Royle et al., 2020) in Appendix S2: Figure S2. In the Montouto-Faro pack, we identified 16 individuals (11 adults; 6 ♂ and 5 ♀; and 5 pups), and in the Bidueiros-Eiras pack, we identified 6 individuals (6 adults; 4 ♂ and 2 ♀). We detected only one breeding female in each pack. None of the wolves from one pack were detected in the camera traps in which the other pack was detected (Figure 1; Appendix S2: Figure S2). We also detected three lone individuals in the Montouto-Faro area (see Appendix S1) who never appeared with other wolves in the video captures, and showed no known associations with other wolves at any time during the study. These lone individuals probably did not belong to either pack and were considered to be floating individuals. The most detected individuals were both reproductive males (*Coxo* from the Montouto-Faro pack, with 65 detections and *Foxo* from the Bidueiros-Eiras pack, with 76 detections) and the fewest detections were of floating individuals (1–5 events) and pups (2–7 events). Pups were only seen at two camera traps (125 m apart), while the rest of the pack members each appeared at an average of 6.8 camera traps. Floating wolves were detected at an average of 2.3 camera traps. The overall wolf activity was mainly nocturnal (Figure 3), although 9% of the events were diurnal, and these detections greatly facilitated the identification of individuals. In our proxy for cohesion, 35% of the trap-days only detected one individual, and 86% of the trap-days detected fewer than five individuals. In 1% of the trap-days, more than 10 individuals were recorded (see Appendix S2: Figure S3).

The convergence of the MCMC chains was good for all models tested, although the chains were poorly mixed in the case of P-$\varepsilon_{ijk}$. According to the WAIC procedure, the best fit model was P-$\varepsilon_{ij}$ (Poisson with a random effect by individual by trap), and the second one was NB-$\varepsilon_j$ (NB observation model with a random effect on the basal detection rate), but P-$\varepsilon_{ij}$ had a severe lack of fit in the "trap" component (Table 1). Therefore, we decided to use NB-$\varepsilon_j$. The difficulties of model selection using WAIC in SCR analysis (Dey et al., 2019), and the additional use of GoF (Jiménez et al., 2022), have been described previously. The estimate of wolf density was 2.88 (SD: 0.37) individuals/100 km$^2$. The population size estimate using

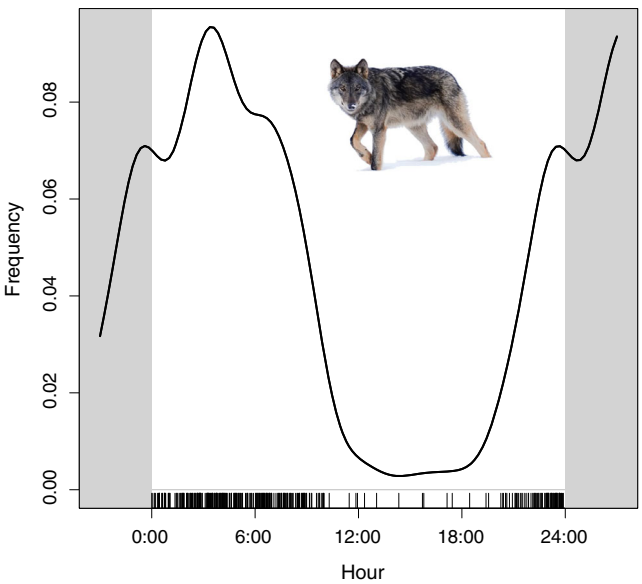


**FIGURE 3** Patterns of wolf activity in the study area. Wolf video captures during daylight hours facilitated the process of individual identification (photo credit: Carlos Usamentiaga: www.ferus.es).

a buffer of 10.45 km ($3 \times \sigma$) around the camera traps was 28.97 (SD: 3.68) individuals (Table 2). The statistics used in the GoF resulted in individual × trap frequencies of $T_1 = 0.56$; individual frequencies of $T_2 = 0.42$, and trap frequencies of $T_3 = 0.20$ (Figure 4).

The data dilution test showed a mean RMSE of the $D$ estimate: for 337 detections (60% of our data) of 0.25 (SD: 0.19) and for 112 detections (20% of our data) of 0.57 (SD: 0.41). The mean RB was 0.07 (SD: 0.09) and 0.18 (SD: 0.18) in 60% and 20% of the cases, respectively (Figure 5).

**TABLE 1** Comparison of the candidate models used to analyze the spatial capture–recapture data: P (Poisson observation model and constant baseline detection rate), P-$\varepsilon_i$, P-$\varepsilon_j$, P-$\varepsilon_{ij}$, and P-$\varepsilon_{ijk}$ (Poisson observation model and random effects on baseline detection rate at individual, trap, individual-trap, and individual-trap-occasion levels, respectively), NB, and NB-$\varepsilon_j$ (negative binomial observation model and a negative binomial and a trap-level random effect on baseline detection rate).

| Model | $T_1$ | $T_2$ | $T_3$ | WAIC |
|---|---|---|---|---|
| Negative binomial (NB-$\varepsilon_j$) | 0.56 | 0.42 | 0.20 | 899.99 |
| Negative binomial (NB) | 0.88 | 0.47 | 0.00 | 995.84 |
| Poisson (P-$\varepsilon_{ij}$) | 0.32 | 0.43 | 0.00 | 847.87 |
| Poisson (P-$\varepsilon_j$) | 0.00 | 0.33 | 0.25 | 930.40 |
| Poisson (P-$\varepsilon_i$) | 0.00 | 0.42 | 0.00 | 1153.07 |
| Poisson (P) | 0.00 | 0.39 | 0.00 | 1174.64 |
| Poisson (P-$\varepsilon_{ijk}$) | 0.00 | 0.08 | 0.00 | 5663.73 |

*Note*: Bayesian $p$ values statistics to evaluate the observation model: ($T_1$) Individual per detector frequencies, ($T_2$) individual detection frequencies, and ($T_3$) trap detection frequencies.
Abbreviation: WAIC, widely applicable information criterion.

## DISCUSSION

The identification of wolves based on their physical characteristics and behavior is not a novel approach. Murie (1944) described how it was possible to differentiate wolves in a pack based on their color, size, contour, and behavior, and included their temperament as a distinguishing feature. It is possible to identify individual wolves from camera trap videos in many cases by observing certain morphological characteristics, injuries, and behaviors. To optimize identification, videos should be taken from a distance of 3–4 m to enable detailed observations, and lures should be used to keep animals in front of the camera for a sufficiently long period of time (Tourani et al., 2020) to enable recordings from various angles, although, as discussed later, baits could induce trap response behavior. Events recorded during the daytime also facilitate the creation of a catalog from which individuals can be identified. The activity patterns we observed (Figure 3) were indicative of the high quality of the videos that we obtained. However, even with daytime photos and videos, the difficulty of identifying individual wolves must be emphasized. The operator(s) performing the identification must develop expertise in this task. It is very difficult to do this without a thorough knowledge of the anatomy and behavior of the species, and the impact of identification errors on the estimates (Johansson et al., 2020) must be addressed in further research. The

**TABLE 2** Posterior summaries of parameters from models P (Poisson observation model and constant baseline detection rate), P-$\varepsilon_i$, P-$\varepsilon_j$, P-$\varepsilon_{ij}$, and P-$\varepsilon_{ijk}$ (Poisson observation model and a random effects on baseline detection rate at individual, trap, individual-trap, and individual-trap-occasion levels, respectively), NB, and NB-$\varepsilon_j$ (negative binomial observation model and a negative binomial and a trap-level random effect on baseline detection rate) used to estimate wolf density.

| Parameter | P | P-$\varepsilon_i$ | P-$\varepsilon_j$ | P-$\varepsilon_{ij}$ | P-$\varepsilon_{ijk}$ | NB | NB-$\varepsilon_j$ |
|---|---|---|---|---|---|---|---|
| $\widehat{N}$ | 26.01 (1.83) | 27.95 (4.03) | 31.01 (4.17) | 28.00 (3.66) | 31.03 (3.50) | 27.01 (3.05) | 28.97 (3.68) |
| $\widehat{D}$ | 2.58 (0.18) | 2.78 (0.40) | 3.08 (0.41) | 2.78 (0.36) | 3.08 (0.35) | 2.68 (0.30) | 2.88 (0.37) |
| $\widehat{r}$ | ... | ... | ... | ... | | 0.01 (0.00) | 0.04 (0.01) |
| $\widehat{\sigma}$ | 3.91 (0.22) | 3.75 (0.21) | 3.16 (0.31) | 3.57 (0.30) | 3.28 (0.19) | 3.65 (0.27) | 3.44 (0.31) |
| $\widehat{\lambda}_0$ | 0.16 (0.02) | ... | ... | ... | ... | 0.15 (0.05) | ... |
| $\widehat{\mu}_0$ | ... | −2.08 (0.42) | −2.96 (0.37) | −2.55 (0.26) | −4.80 (0.16) | ... | −2.76 (0.39) |
| $\widehat{\sigma}_p$ | ... | 0.95 (0.47) | 1.62 (0.37) | 1.18 (0.12) | 1.82 (0.10) | ... | 1.41 (0.35) |
| $\widehat{\psi}$ | 0.33 (0.06) | 0.37 (0.07) | 0.40 (0.07) | 0.37 (0.07) | 0.39 (0.07) | 0.36 (0.27) | 0.37 (0.07) |

*Note*: The mode was used as a point estimate. Parameters: $\widehat{N}$ is the population size estimate in a territory buffering all traps using a distance of $3 \times \widehat{\sigma}$; $\widehat{D}$ is the density estimate (individuals/100 km$^2$); $\widehat{r}$ is the negative binomial parameter; $\widehat{\sigma}$ is the half-normal scale parameter describing the rate at which the detection probability declines as a function of distance from the detector; $\widehat{\lambda}_0$ is the baseline detection rate; $\widehat{\mu}_0$ and $\widehat{\sigma}_p$ are the hyperparameters from the random effects; and $\widehat{\psi}$ is the parameter for data augmentation. The mode and SD are shown for all parameters.

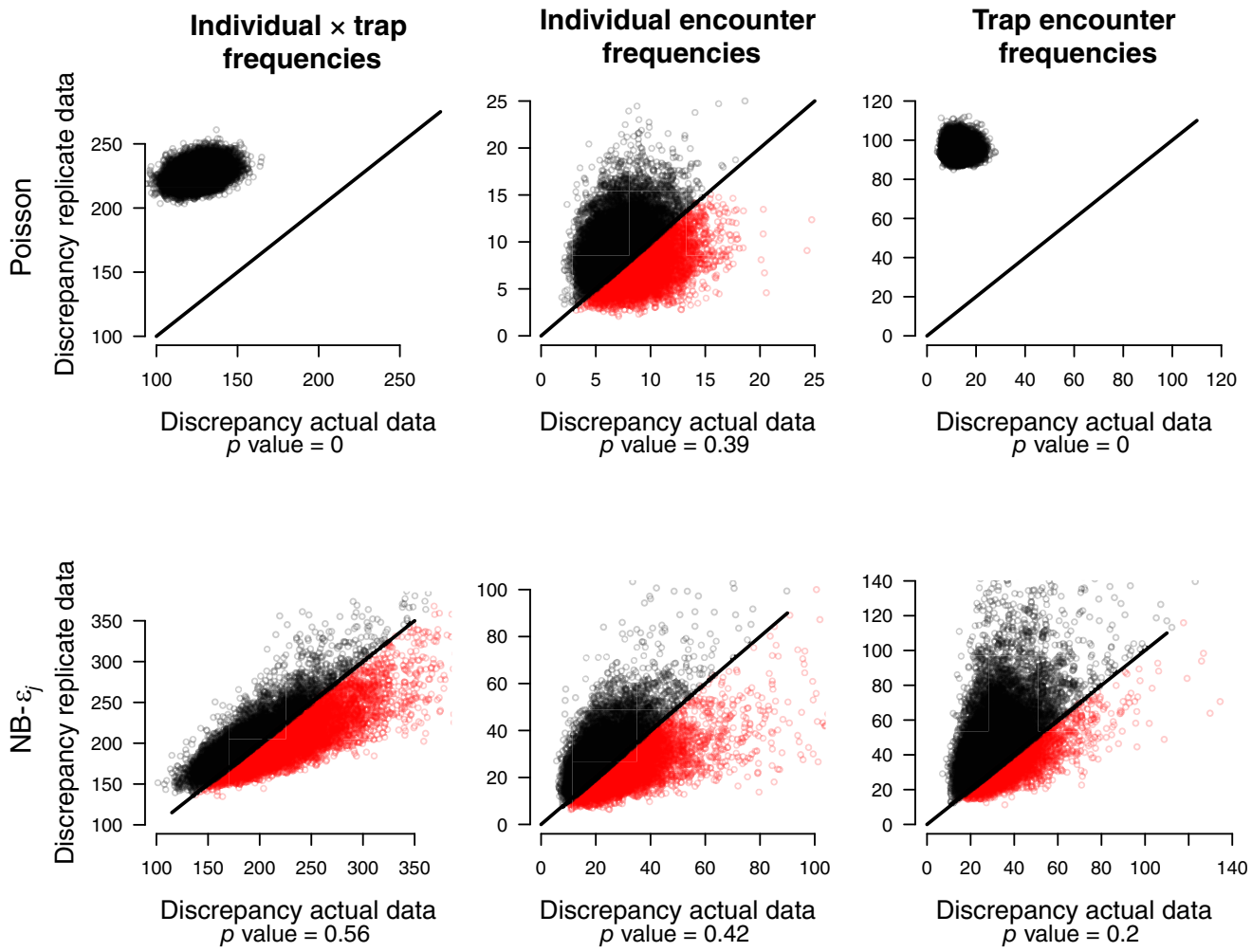


**FIGURE 4** Scatter plots of discrepancy measures for the replicate versus the actual data for the spatial capture–recapture models studied. Top, Poisson model and bottom, negative binomial with random effects by traps on basal detection rate (NB-$\varepsilon_j$). The Bayesian *p* values are the proportion of points below the 1:1 equality line (black). Left: individual × trap frequencies, which summarize the data by individual and camera trap, aggregated over a single occasion. Center: individual detection frequencies, which assess individual heterogeneity. Right: camera trap frequencies, based on aggregating individuals and replicates to create camera trap/detection frequencies.

minimum detected population size (MDS) in the study area was 28 individuals: 25 identified during the study period, one pup from the Montouto-Faro pack that was found dead during the study but prior to detecting the pups in camera traps, and two pups discovered later in the Bidueiros-Eiras pack. Given the intensive monitoring of this population, the MDS could be considered a good baseline for comparing estimates.

By moving the cameras and changing their location, it was possible to cover the entire sampling area. It should be noted that it was necessary to have enough detections and recaptures in different locations that are far enough apart to allow for a correct estimation of σ. For example, only using cameras at rendezvous sites could maximize the number of captures/recaptures, but would not enable a description of the actual movement of animals. For this particular type of spatial distribution of a population, spatially clustered and over a large area, it may be desirable to use adaptive sampling (Wong et al., 2018) and model it appropriately. It should be noted that adaptive sampling with a standard SCR analysis will result in an overestimation of the population size.

While breeding females in a pack are easily identified by the presence of mammary glands at this time of year, the larger wolves that often appear in video captures simultaneously with breeding females could be only be considered as putative breeding males. Two wolves from the dataset, *Coxo* (No. 2) and *Foxo* (No. 21), were detected in company with the reproductive females *Deva* (No. 1) and *Laxe* (No. 20) in 27 and 31 video captures, respectively, and apparently guided the pack activity (Mech, 2000). In our study, direct observations of wolves, made

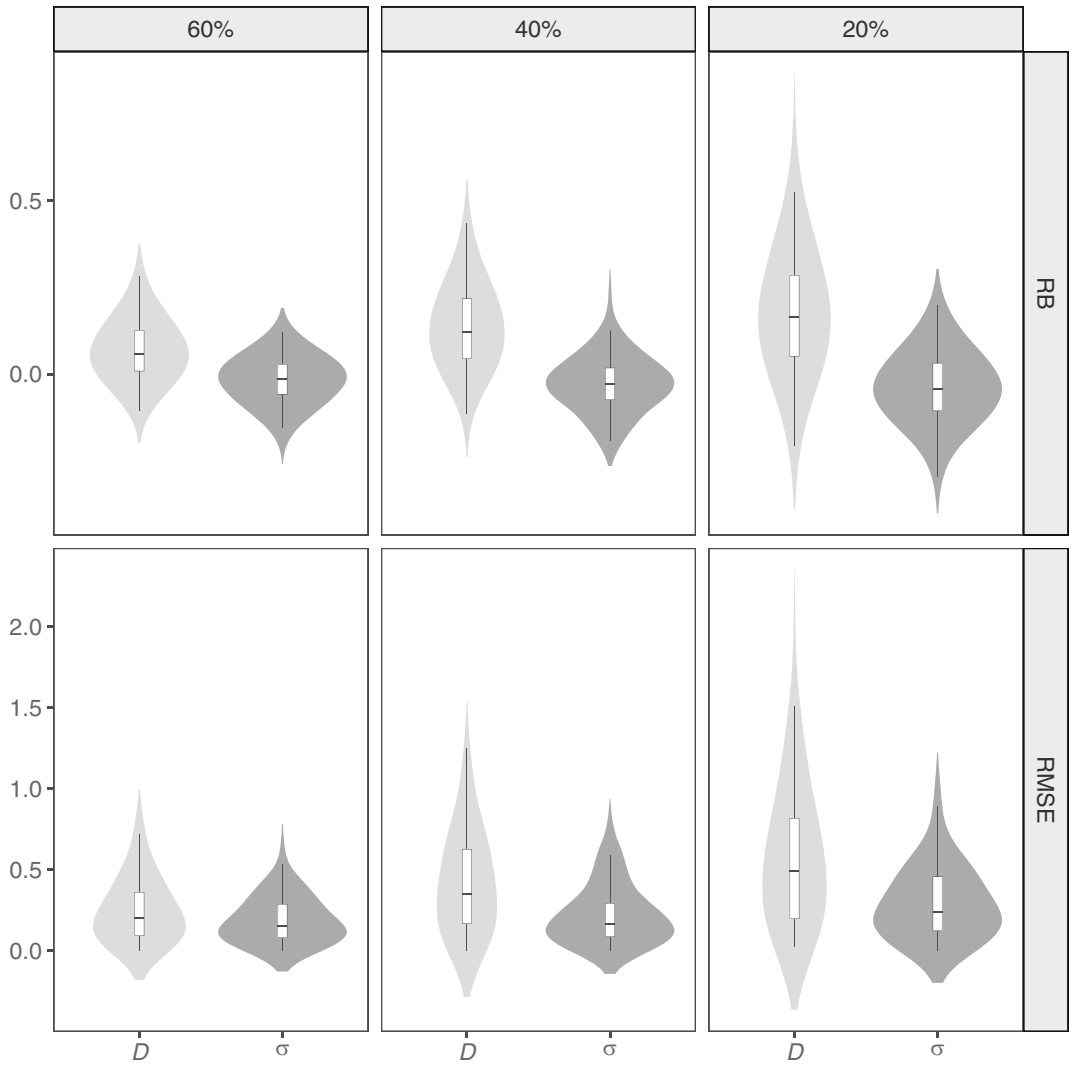


**FIGURE 5** Relationships between sample size and root-mean-square error (RMSE) and relative bias (RB) of density ($D$) and sigma ($\sigma$) from the NB-$\varepsilon_j$ spatially explicit capture–recapture model, under three dilution scenarios and 100 simulated datasets per scenario: 60% (337 detections), 40% (225), and 20% (112) of the data. Violins represent the parameter distribution in each dilution scenario.

at several locations without disturbing them, confirmed that *Coxo* and *Foxo* were in fact breeding males.

Considering the individuals recognized during the study period, 16 individuals belonged to the Montouto-Faro pack, six belonged to the Bidueiros-Eiras pack, and three were floating individuals. The size of the Montouto-Faro pack is abnormally high for Spain. Fernández-Gil et al. (2020) reported an average of 3.1 (SD: 1.3) adult/subadult individuals (older than one year) at summer rendezvous sites and an average of 4.0 (SD: 1.9) individual pups. The larger Montouto-Faro pack was particularly advantageous to the objective of our study, since, a priori, larger pack sizes will result in larger biases if aggregation and cohesion are not included in the model (Bischof, Dupont, et al., 2020). We found that 12% of the wolves observed were not linked to breeding packs during the summer. Although our sample size was small, the percentage of floating wolves was slightly lower than the 16%–25% calculated in the study by López-Bao et al. (2018) and was similar to figures estimated for North American populations (7%–20%) (Mech & Boitani, 2006).

Although the a priori hypothesis was that gregariousness would be modeled using a random effect by individual-by-trap-by occasion, we found that the GoF was better with an NB model with a random effect by trap. In fact, this does not contradict our initial hypothesis, since the NB model alone accounts for the heterogeneity individual-by-trap-by-occasion. Additionally, in our analysis, the GoF test did not detect a lack of fit in the NB-$\varepsilon_j$ model, as the BPVs were not close to 0 or 1 for any of the components, suggesting that the heterogeneity was well explained by this model (Figure 4), in contrast to the lack of fit detected in other models. By adding an additional heterogeneity by trap, we reinforce this dimension

of heterogeneity. Thus, it is possible that the better fit of the NB model with a random effect by trap is related to other sources of heterogeneity besides that induced by gregariousness. The lack of fit in the third component of the P-$\varepsilon_{ij}$ model also suggests unresolved trap heterogeneity in this model. The population size $N$ of individuals estimated by the P, P-$\varepsilon_i$, and NB models are lower than the MDS, while the $N$ estimated by P-$\varepsilon_{ij}$ is the same, and for P-$\varepsilon_j$, P-$\varepsilon_{ijk}$ and NB-$\varepsilon_j$ are slightly higher than the MDS. There are also differences in the σ values estimated by the different models. The relationship between $\lambda_0$ and σ can compensate between parameters (Efford & Mowat, 2014). Thus, if there was any unmodeled overdispersion in our data using P (as suggested by the GoF), we might expect unrealistically high σ estimates. Indeed, comparing the mean of our $\widehat{\sigma}$ estimates with those obtained from the GPS-telemetry data in López-Bao et al. (2018) for a sample of 16 GPS-tagged individuals from the same population in Galicia ($\sigma_{tel} = 3.50$ km), it suggests an overestimation in the scale parameter estimates in models P ($\widehat{\sigma}_P = 3.92$ km), P-$\varepsilon_i$ ($\widehat{\sigma}_{P\text{-}\varepsilon_i} = 3.75$ km), NB ($\widehat{\sigma}_{NB} = 3.67$), and P-$\varepsilon_{ij}$ ($\widehat{\sigma}_{P\text{-}\varepsilon_{ij}} = 3.57$ km). All of these models had a lack of fit in $T_3$, and P and P-$\varepsilon_i$ also had a lack of fit in $T_1$. The mean estimate of the selected NB-$\varepsilon_j$ model ($\widehat{\sigma}_{NB\text{-}\varepsilon_j} = 3.50$ km) was the same as $\sigma_{tel}$. Compensatory heterogeneity in P leads to an overestimation of σ and an underestimation of the density in the state space, which in our case was 10.4% when comparing P and NB-$\varepsilon_j$; 2.58 (SD: 0.18) versus 2.88 (0.37) individuals/100 km$^2$, respectively. As expected, the SD estimate could also be unrealistically small due to unmodeled overdispersion in P (Anderson et al., 1994). The estimate of the P-$\varepsilon_j$ model ($\widehat{\sigma}_P = 3.26$ km) and the P-$\varepsilon_{ijk}$ model ($\widehat{\sigma}_{P\text{-}\varepsilon_{ijk}} = 3.33$ km) is lower than $\sigma_{tel}$, and both models had a lack of fit in $T_1$, and P-$\varepsilon_{ijk}$ also had a lack of fit in $T_3$. We can infer that there is heterogeneity in our wolf data in the three components: individual by trap ($T_1$), individual ($T_2$), and trap ($T_3$), but the heterogeneity of the trap component appears to be greater. The NB observation model with an additional trap-level random effect, which better accommodates this component, has the best BPV.

The difference between the four packs estimated in a previous study in 2013–2014 (MITECO, 2015) and the two packs detected in this study (2015) could be due to a reduction in the population, a restructuring of the pack compositions for some unknown reason, or differences arising from the methodology used. In any case, we would expect the level of accuracy obtained using our camera traps, individual identification, and capture–recapture approaches to be higher (Pollock, 1976) than that achieved using other methods.

With regard to the "subsampling" process that occurs when considering only a portion of the events, it should be noted that, if subsampling is random with respect to individuals, we would observe a greater reduction in the $\lambda_0$ value than if we used all of the identified events, albeit with more bias and a less precise estimate as the number of unidentified events increases (Figure 5). However, if the subsampling process that occurs when identifying individuals from the videos is not random (e.g., if some individuals are more identifiable than others), individual heterogeneity will be introduced in $\lambda_0$. Where this problem is suspected, it can be addressed by removing individual heterogeneity in detection by combining the random thinning spatial capture–recapture model (Jiménez et al., 2021) with the categorical SCR model (Augustine et al., 2019) as described by Cove et al. (2023). Another problem could arise if there were behavioral responses to the traps, because we cannot be sure whether some of the wolves detected (and identified) in one event might actually be present, but unidentified, in a previous video event. Therefore, although it might be plausible that the bait induced a capture response in our sampling, the behavioral response model ($M_b$) was not included in our analyses. When using nonspatial capture–recapture methods, estimates can become very biased when combined with subsampling (Augustine et al., 2014); however, in studies using SCR, there have been reports of limited effects on the estimate when other sampling methodologies (genetic noninvasive sampling) were used (Murphy et al., 2016). Response behavior in data with a subsampling process could be addressed using the random thinning SCR model (Jiménez et al., 2021), but incorporating a behavioral response to capture. It should also be noted that in our data dilution experiments, which are actually an additional subsampling to the identification process (Figure 5), the bias increased with increasing dilution, suggesting that smaller sample sizes may limit the accuracy of the predictions. This problem is likely caused by the distribution of our cameras, where random dilution may lead to an underestimation of σ by eliminating some of the few more spatially distant recaptures (Appendix S2: Figure S2), resulting in an overestimation of density.

It is important to emphasize that although the differences between the models studied may not be very important due to the high cumulative capture probability of each individual in our data, they will be important in other studies with lower capture rates, as is common in SCR studies. We recommend: (1) sampling during periods of the year in which less cohesive behavior can be expected; (2) accounting for heterogeneity; comparing models with different random effects and observation process; and (3) testing the GoF of the models. The NB model with random effects on the basal detection rate will be adequate if we found aggregation and cohesion behavior and other sources of heterogeneity similar to our case

study. Judging by the data, the packs we studied were not very cohesive (see Appendix S2: Figure S3) in this area during the study period, and usually split into several groups at various times. If pack behavior becomes more cohesive or there are other heterogeneity sources, this approach may not be enough to address the resulting overdispersion. In these cases, other types of random effects (Dey et al., 2023) or using nonparametric ones (Turek et al., 2021) could be considered.

Can this method of estimating wolf density be extrapolated to larger landscape scales in NW Spain? Probably not. The selection of the study area was arbitrary and only covered an area occupied by two packs. It is possible that at a larger scale, the average density would be lower due to the inclusion of areas of wolf low density, or an absence of wolves altogether (Fuller & Murray, 1998). As a reference for comparison, López-Bao et al. (2018) estimated 2.55 (SD: 0.42) individuals/100 km$^2$ using a Poisson observation model. The analytical procedures used in this study could be replicated at a medium scale, because cataloging and comparing images "by eye" is difficult in large populations. Our method allows the use of covariates such as social or reproductive status, response to camera traps (with the caution noted above), gregariousness, and so forth, which are difficult (or expensive) to detect with noninvasive genetic procedures. Furthermore, camera trap data provide valuable information on the health status of a population, its behavior, etc. A similar study scheme, ideally incorporating adequate sampling, individual recognition in camera trap videos, SCR modeling that takes into account overdispersion through different observation models and random effects, model selection, and performing GoF tests, could be applied to other gregarious species.

## AUTHOR CONTRIBUTIONS

*Conceptualization*: José Jiménez. *Formal analysis*: José Jiménez. Methodology: José Jiménez. *Software*: José Jiménez. *Writing—original draft*: José Jiménez. *Data curation*: Daniel Cara, Francisco García Domínguez, and Jose Angel Barasona. *Investigation*: Daniel Cara, Francisco García Domínguez, and Jose Angel Barasona. *Writing—review and editing*: Daniel Cara, Francisco García Domínguez, and Jose Angel Barasona. *Project administration*: Francisco García Domínguez. *Supervision*: Francisco García Domínguez.

## ACKNOWLEDGMENTS

This study was funded by Ministerio para la Transición Ecológica y el Reto Demográfico (MITECO), and Xunta de Galicia facilitated the fieldwork. We are grateful to Ben Augustine for fruitful discussions and comments. We thank Pablo Ferreras for comments on a draft. We also thank the anonymous reviewers who provided constructive comments and suggestions that improved this manuscript. Finally, we thank Andrew Richford for English language editing and checking. Any use of product names in this study is for descriptive purposes only and does not imply endorsement.

## CONFLICT OF INTEREST STATEMENT

The authors declare no conflicts of interest.

## DATA AVAILABILITY STATEMENT

The data and code (Jiménez, 2023) are available in the Zenodo repository at https://zenodo.org/record/7975329.

## ORCID

*José Jiménez* https://orcid.org/0000-0003-0607-6973
*Jose Angel Barasona* https://orcid.org/0000-0003-4066-8454

## REFERENCES

Anderson, D. R., K. P. Burnham, and G. C. White. 1994. "AIC Model Selection in Overdispersed Capture-Recapture Data." *Ecology* 75: 1780–93.

Anscombe, F. J. 1950. "Sampling Theory of the Negative Binomial and Logarithmic Series Distributions." *Biometrika* 37: 358–82.

Augustine, B. C., J. A. Royle, S. M. Murphy, R. B. Chandler, J. J. Cox, and M. J. Kelly. 2019. "Spatial Capture–Recapture for Categorically Marked Populations with an Application to Genetic Capture–Recapture." *Ecosphere* 10: e02627.

Augustine, B. C., C. A. Tredick, and S. J. Bonner. 2014. "Accounting for Behavioural Response to Capture when Estimating Population Size from Hair Snare Studies with Missing Data." *Methods in Ecology and Evolution* 5: 1154–61.

Bischof, R., P. Dupont, C. Milleret, J. Chipperfield, and J. A. Royle. 2020. "Consequences of Ignoring Group Association in Spatial Capture–Recapture Analysis." *Wildlife Biology* 2020: 1–10.

Bischof, R., C. Milleret, P. Dupont, J. Chipperfield, M. Tourani, A. Ordiz, P. de Valpine, et al. 2020. "Estimating and Forecasting Spatial Population Dynamics of Apex Predators Using Transnational Genetic Monitoring." *Proceedings of the National Academy of Sciences of the United States of America* 117: 30531–8.

Bullard, R. W. 1982. "Wild Canid Associations with Fermentation Products." *Industrial and Engineering Chemistry Product Research and Development* 21: 646–55.

Cove, M. V., V. Herrmann, D. J. Herrera, B. C. Augustine, D. T. T. Flockhart, and W. J. McShea. 2023. "Counting the Capital's Cats: Estimating Drivers of Abundance of Free-Roaming Cats with a Novel Hierarchical Model." *Ecological Applications* 33: e2790.

de Valpine, P., C. J. Paciorek, D. Turek, N. Michaud, C. Anderson-Bergman, F. Obermeyer, A. Cortes, C. Wehrhahn Rodrìguez, D. T. Lang, and S. Paganin. 2022. "NIMBLE: MCMC, Particle Filtering, and Programmable Hierarchical Modeling." https://doi.org/10.5281/zenodo.1211190.

de Valpine, P., D. Turek, C. J. Paciorek, D. Anderson-Bergman, T. Lang, and R. Bodik. 2017. "Programming with Models: Writing Statistical Algorithms for General Model Structures with NIMBLE." *Journal of Computational and Graphical Statistics* 26: 403–13.

Dey, S., M. Delampady, and A. M. Gopalaswamy. 2019. "Bayesian Model Selection for Spatial Capture–Recapture Models." *Ecology and Evolution* 9: 11569–83.

Dey, S., E. Moqanaki, C. Milleret, P. Dupont, M. Tourani, and R. Bischof. 2023. "Modelling Spatially Autocorrelated Detection Probabilities in Spatial Capture-Recapture Using Random Effects." *Ecological Modelling* 479: 110324.

Domínguez, G., A. Espí, J. M. Prieto, and J. A. De La Torre. 2008. "Sarcoptic Mange in Iberian Wolves (*Canis lupus signatus*) in Northern Spain." *Veterinary Record* 162: 754–5.

Efford, M. G., D. K. Dawson, and C. S. Robbins. 2004. "DENSITY: Software for Analysing Capture-Recapture Data from Passive Detector Arrays." *Animal Biodiversity and Conservation* 27: 217–28.

Efford, M. G., and G. Mowat. 2014. "Compensatory Heterogeneity in Spatially Explicit Capture-Recapture Data." *Ecology* 95: 1341–8.

Emmet, R. L., B. C. Augustine, B. Abrahms, L. N. Rich, and B. Gardner. 2022. "A Spatial Capture–Recapture Model for Group-Living Species." *Ecology* 103: 33576.

Fernández-Gil, A., M. Quevedo, L. M. Barrientos, A. Nuño, J. Naves, M. De Gabriel, A. Ordiz, and E. Revilla. 2020. "Pack Size in Humanized Landscapes: The Iberian Wolf Population." *Wildlife Biology* 2020: 1–9.

Fuller, T. K., and D. L. Murray. 1998. "Biological and Logistical Explanations of Variation in Wolf Population Density." *Animal Conservation* 1: 153–7.

Gelman, A., J. B. Carlin, H. S. Stern, D. B. Dunson, A. Vehtari, and D. B. Rubin. 2013. *Bayesian Data Analysis*, 3rd ed. Boca Raton, FL: CRC Press.

Gelman, A., X. L. Meng, and H. Stern. 1996. "Posterior Predictive Assessment of Model Fitness Via Realized Discrepancies." *Statistica Sinica* 6: 733–807.

Harrison, X. A. 2014. "Using Observation-Level Random Effects to Model Overdispersion in Count Data in Ecology and Evolution." *PeerJ* 2: e616.

Havmøller, R. W., S. Tenan, N. Scharff, and F. Rovero. 2019. "Reserve Size and Anthropogenic Disturbance Affect the Density of an African Leopard (*Panthera pardus*) Meta-Population." *PLoS One* 14: e0209541.

INE. 2018. "Sociedad." http://www.ine.es/dyngs/INEbase/es/categoria.htm?c=Estadistica_P&cid=1254735971047.

Jiménez, J. 2023. "JoseJimenezGH/DorsalGallega_Wolves: DorsalGallega_Wolves." Zenodo. https://zenodo.org/record/7975329.

Jiménez, J., B. C. Augustine, D. W. Linden, R. B. Chandler, and J. A. Royle. 2021. "Spatial Capture–Recapture with Random Thinning for Unidentified Encounters." *Ecology and Evolution* 11: 1187–98.

Jiménez, J., E. J. García, L. Llaneza, V. Palacios, L. M. González, F. García-Domínguez, J. Muñoz-Igualada, and J. V. López-Bao. 2016. "Multimethod, Multistate Bayesian Hierarchical Modeling Approach for Use in Regional Monitoring of Wolves." *Conservation Biology* 30: 883–93.

Jiménez, J., R. Godinho, D. Pinto, S. Lopes, D. Castro, D. Cubero, M. A. Osorio, et al. 2022. "The Cantabrian Capercaillie: A Population on the Edge." *Science of the Total Environment* 821: 153523.

Jiménez, J., J. C. Nuñez-Arjona, C. Rueda, L. M. González, F. García-Domínguez, J. Muñoz-Igualada, and J. V. López-Bao. 2017. "Estimating Carnivore Community Structures." *Scientific Reports* 7: 1–10.

Johansson, Ö., G. Samelius, E. Wikberg, and G. Chapron. 2020. "Identification Errors in Camera-Trap Studies Result in Systematic Population Overestimation." *Scientific Reports* 10: 6393.

Jumeau, J., L. Petrod, and Y. Handrich. 2017. "A Comparison of Camera Trap and Permanent Recording Video Camera Efficiency in Wildlife Underpasses." *Ecology and Evolution* 7: 7399–407.

Kéry, M., and M. Schaub. 2012. *Bayesian Population Analysis using WinBUGS. A Hierarchical Perspective*. Waltham, MA: Academic Press/Elsevier.

López-Bao, J. V., R. Godinho, C. Pacheco, F. J. Lema, E. García, L. Llaneza, V. Palacios, and J. Jiménez. 2018. "Toward Reliable Population Estimates of Wolves by Combining Spatial Capture-Recapture Models and Non-Invasive DNA Monitoring." *Scientific Reports* 8: 2177.

Mattioli, L., A. Canu, D. Passilongo, M. Scandura, and M. Apollonio. 2018. "Estimation of Pack Density in Grey Wolf (*Canis lupus*) by Applying Spatially Explicit Capture-Recapture Models to Camera Trap Data Supported by Genetic Monitoring." *Frontiers in Zoology* 15: 1–15.

Mech, L. D. 2000. "Leadership in Wolf, *Canis lupus*, Packs." *Canadian Field-Naturalist* 114: 259–63.

Mech, L. D., and L. Boitani. 2006. *Wolves: Behavior, Ecology, and Conservation*. Chicago, IL: University of Chicago Press.

MITECO. 2015. "Resultados del Censo Nacional 2012–2014 del lobo ibérico (*Canis lupus*) en España." https://www.miteco.gob.es/en/biodiversidad/temas/inventarios-nacionales/censo_lobo_espana_2012_14pdf_tcm38-197304.pdf.

Murie, A. 1944. *The Wolves of Mount MacKinley*. Washington, DC: Fauna of the National Parks of the United States. Fauna Series no. 5. Department of the Interior, National Park Service, United States.

Murphy, S. M., B. C. Augustine, J. R. Adams, L. P. Waits, and J. J. Cox. 2018. "Integrating Multiple Genetic Detection Methods to Estimate Population Density of Social and Territorial Carnivores." *Ecosphere* 9: e02479.

Murphy, S. M., J. J. Cox, B. C. Augustine, J. T. Hast, J. M. Guthrie, J. Wright, J. McDermott, S. C. Maehr, and J. H. Plaxico. 2016. "Characterizing Recolonization by a Reintroduced Bear Population Using Genetic Spatial Capture–Recapture." *Journal of Wildlife Management* 80: 1390–407.

Newsome, T. M., and W. J. Ripple. 2015. "A Continental Scale Trophic Cascade from Wolves through Coyotes to Foxes." *Journal of Animal Ecology* 84: 49–59.

Oleaga, Á., R. Casais, A. Balseiro, A. Espí, L. Llaneza, A. Hartasánchez, and C. Gortázar. 2011. "New Techniques for an Old Disease: Sarcoptic Mange in the Iberian Wolf." *Veterinary Parasitology* 181: 255–66.

Plummer, M., N. Best, K. Cowles, and K. Vines. 2006. "CODA: Convergence Diagnosis and Output Analysis for MCMC." *R News* 6: 7–11.

Pollock, K. H. 1976. "Building Models of Capture-Recapture Experiments." *The Statistician* 25: 253.

Pradel, R., O. Gimenez, and J.-D. Lebreton. 2005. "Principles and Interest of GOF Tests for Multistate Capture–Recapture Models." *Animal Biodiversity and Conservation* 28: 189–204.

R Core Team. 2022. *R: A Language and Environment for Statistical Computing*. Vienna: R Foundation for Statistical Computing. https://www.r-project.org/.

Ridout, M. S., and M. Linkie. 2009. "Estimating Overlap of Daily Activity Patterns from Camera Trap Data." *Journal of Agricultural, Biological, and Environmental Statistics* 14: 322–37.

Ripple, W. J., and R. L. Beschta. 2012. "Trophic Cascades in Yellowstone: The First 15 Years after Wolf Reintroduction." *Biological Conservation* 145: 205–13.

Ripple, W. J., E. J. Larsen, R. A. Renkin, and D. W. Smith. 2001. "Trophic Cascades among Wolves, Elk and Aspen on Yellowstone National Park's Northern Range." *Biological Conservation* 102: 227–34.

Roffler, G. H., J. N. Waite, K. L. Pilgrim, K. E. Zarn, and M. K. Schwartz. 2019. "Estimating Abundance of a Cryptic Social Carnivore Using Spatially Explicit Capture-Recapture." *Wildlife Society Bulletin* 43: 1–11.

Royle, J. A., R. B. Chandler, R. Sollmann, and B. Gardner. 2014. *Spatial Capture-Recapture*. Waltham, MA: Elsevier, Academic Press.

Royle, J. A., R. B. Chandler, R. Sollmann, and B. Gardner. 2020. "scrbook: Companion to the Book: Spatial Capture Recapture (2014)." R Package Version 0.31-0.

Royle, J. A., R. M. Dorazio, and W. A. Link. 2007. "Analysis of Multinomial Models with Unknown Index Using Data Augmentation." *Journal of Computational and Graphical Statistics* 16: 67–85.

Royle, J. A., and K. V. Young. 2008. "A Hierarchical Model for Spatial Capture-Recapture Data." *Ecology* 92: 526–8.

Schmidt, P. A., and L. D. Mech. 1997. "Wolf Pack Size and Food Acquisition." *The American Naturalist* 150: 513–7.

Tourani, M., E. N. Brøste, S. Bakken, J. Odden, and R. Bischof. 2020. "Sooner, Closer, or Longer: Detectability of Mesocarnivores at Camera Traps." *Journal of Zoology* 312: 259–70.

Turek, D., C. Wehrhahn, and O. Gimenez. 2021. "Bayesian Non-parametric Detection Heterogeneity in Ecological Models." *Environmental and Ecological Statistics* 28: 355–81.

Vucetich, J. A., R. O. Peterson, and T. A. Waite. 2004. "Raven Scavenging Favours Group Foraging in Wolves." *Animal Behaviour* 67: 1117–26.

Watanabe, S. 2013. "A Widely Applicable Bayesian Information Criterion." *Journal of Machine Learning Research* 14: 867–97.

Williams, B. K., J. D. Nichols, and M. J. Conroy. 2002. *Analysis and Management of Animal Populations: Modeling, Estimation, and Decision Making*. San Diego, CA: Academic Press.

Wong, A., A. Fuller, and J. A. Royle. 2018. "Adaptive Sampling for Spatial Capture-Recapture: An Efficient Sampling Scheme for Rare or Patchily Distributed Species." *bioRxiv*: 357459.

## SUPPORTING INFORMATION

Additional supporting information can be found online in the Supporting Information section at the end of this article.

**How to cite this article:** Jiménez, José, Daniel Cara, Francisco García-Dominguez, and Jose Angel Barasona. 2023. "Estimating Wolf (*Canis lupus*) Densities Using Video Camera Traps and Spatial Capture–Recapture Analysis." *Ecosphere* 14(7): e4604. https://doi.org/10.1002/ecs2.4604